

# UC Irvine

## UC Irvine Previously Published Works

### Title

Glutamine fuels proliferation but not migration of endothelial cells

### Permalink

<https://escholarship.org/uc/item/1zp848kz>

### Journal

The EMBO Journal, 36(16)

### ISSN

0261-4189

### Authors

Kim, Boa

Li, Jia

Jang, Cholsoon

et al.

### Publication Date


2017-08-15

### DOI

10.15252/emj.201796436

Peer reviewed

# Glutamine fuels proliferation but not migration of endothelial cells

 Boa Kim<sup>1,2,†</sup>, Jia Li<sup>1,2,†</sup>, Cholsoon Jang<sup>1,2,3</sup> & Zoltan Arany<sup>1,2,\*</sup> 

## Abstract

Endothelial metabolism is a key regulator of angiogenesis. Glutamine metabolism in endothelial cells (ECs) has been poorly studied. We used genetic modifications and <sup>13</sup>C tracing approaches to define glutamine metabolism in these cells. Glutamine supplies the majority of carbons in the tricyclic acid (TCA) cycle of ECs and contributes to lipid biosynthesis via reductive carboxylation. EC-specific deletion in mice of glutaminase, the initial enzyme in glutamine catabolism, markedly blunts angiogenesis. In cell culture, glutamine deprivation or inhibition of glutaminase prevents EC proliferation, but does not prevent cell migration, which relies instead on aerobic glycolysis. Without glutamine catabolism, there is near complete loss of TCA intermediates, with no compensation from glucose-derived anaplerosis. Mechanistically, addition of exogenous alpha-ketoglutarate replenishes TCA intermediates and rescues cellular growth, but simultaneously unveils a requirement for Rac1-dependent macropinocytosis to provide non-essential amino acids, including asparagine. Together, these data outline the dependence of ECs on glutamine for cataplerotic processes; the need for glutamine as a nitrogen source for generation of biomass; and the distinct roles of glucose and glutamine in EC biology.

**Keywords** endothelium; glutamine; macropinocytosis; migration

**Subject Categories** Metabolism; Vascular Biology & Angiogenesis

**DOI** 10.15252/emboj.201796436 | Received 3 January 2017 | Revised 26 May 2017 | Accepted 30 May 2017 | Published online 28 June 2017

**The EMBO Journal (2017) 36: 2321–2333**

See also: **H Huang *et al*** (August 2017) and **J Andrade & M Potente** (August 2017)

## Introduction

Endothelial cells (ECs) line the walls of the entire vascular tree, covering up to 2,000 m<sup>2</sup> of area. ECs play critical roles in systemic metabolism, including transport of nutrients and waste between parenchyma and the circulation. ECs themselves also have unique metabolic needs. Most ECs are largely quiescent, with half-lives of

months to years. On the other hand, ECs can be activated to rapidly proliferate by physiologic stimuli like exercise and endometrial cycling, or pathological stimuli like trauma, inflammation, or tumors. In the latter context, ECs often proliferate and migrate into metabolically challenging environments, including ones lacking oxygen or extracellular nutrients. ECs thus share striking functional similarities with tumor cells. Indeed, like tumor cells, ECs consume copious amounts of glucose via glycolysis, without subsequently oxidizing the resulting pyruvate in mitochondria despite the presence of oxygen. De Bock *et al* have measured that ECs generate more than 80% of their ATP through aerobic glycolysis, a phenomenon known in the context of tumor biology as the Warburg effect (De Bock *et al*, 2013; Verdegem *et al*, 2014). EC metabolism may thus share additional similarities with that of tumor cells.

The high glycolytic rate of tumor cells has often been ascribed to the need for carbons for the synthesis of biomass (Vander Heiden *et al*, 2009; Hay, 2016). Another increasingly appreciated source of carbons for biomass synthesis in tumor cells is the amino acid glutamine. Glutamine is the most abundant nonessential amino acid in the human body. Circulating levels range from 400 to 600 μM, the largest concentration of any amino acid (Mayers & Vander Heiden, 2015). Glutamine contributes to various metabolic and biosynthetic pathways. Once imported into the cells, glutamine is converted to glutamate by glutaminase (GLS). Glutamate is then converted to α-ketoglutarate (αKG) which enters the TCA cycle as an anaplerotic source of carbons. TCA intermediates generated from glutamine can also be used to produce various non-essential amino acids needed for cell growth. In addition, the carboxylation of αKG to citrate by isocitrate dehydrogenase (called reductive carboxylation because it occurs in direction opposite to the canonical oxidative progression of the TCA cycle) has been reported in numerous tumor cells (Ward *et al*, 2010; Metallo *et al*, 2011; Mullen *et al*, 2011; Wise *et al*, 2011) and has been suggested as an important source of cytosolic acetyl-CoA for fatty acid synthesis.

Glutamine metabolism in ECs has not been studied extensively. The maximal enzymatic activities of GLS and glutamate dehydrogenase in ECs are quite high, at least an order of magnitude higher than in lymphocytes (Leighton *et al*, 1987), suggesting an important role for glutamine in EC metabolism. In light of the similarities between ECs and various cancer cells, and the established importance of glutamine in cancer cell metabolism, we endeavored to

1 Department of Medicine, Cardiovascular Institute, Perelman School of Medicine, University of Pennsylvania, Philadelphia, PA, USA

2 Institute of Diabetes Obesity and Metabolism, Perelman School of Medicine, University of Pennsylvania, Philadelphia, PA, USA

3 Chemistry and Integrative Genomics, Princeton University, Princeton, NJ, USA

\*Corresponding author. Tel: +1 215 898 3482; E-mail: zarany@mail.med.upenn.edu

†These authors contributed equally to this work

evaluate glutamine metabolism in ECs, and to test the role of glutamine, in cell culture and *in vivo*, in EC proliferation and function.

## Results

Endothelial cells (ECs) are known to be highly glycolytic (De Bock *et al*, 2013; Eelen *et al*, 2015). We measured glucose consumption of human umbilical endothelial cells (HUVECs) in culture as ~8 nmol per 10,000 cells/h (Table 1), a rate comparable to that seen in tumor cells (Li *et al*, 2014). The high glycolytic rate of tumor cells has often been ascribed to the need for carbons for the synthesis of biomass (Vander Heiden *et al*, 2009; Hay, 2016). However, we found that the glycolytic index of HUVECs, defined as glucose consumed divided by lactate produced, was 1.74, indicating that nearly 90% of carbons entering the cell as glucose are subsequently exiting the cell as lactate (Table 1). ECs therefore must use alternate sources of carbons for synthesis of biomass.

The consumption of glutamine, known to be high in tumor cells (Mullen *et al*, 2011; Altman *et al*, 2016), has not been studied extensively in ECs. We measured glutamine consumption of HUVECs as ~2 nmol per 10,000 cells/h (Table 1). In sharp contrast to glucose, 90% of the glutamine remained in the cell, with only a small fraction escaping as glutamate (glutamine index of 0.10, Table 1). Glutamine can therefore contribute at least twice as many carbons to biomass as glucose.

Glutamine consumption in cells occurs largely by conversion to glutamate (via GLS) followed by either de-amination or transamination to aKG, which then enters the tricyclic acid (TCA) cycle. We used stable isotope tracing techniques to determine the contributions of glucose and glutamine to TCA cycle intermediates (Fig 1A). HUVECs maintained in media containing [U-<sup>13</sup>C] glutamine revealed more than 70% labeling of carbons in the TCA cycle, while cells maintained in the presence of [U-<sup>13</sup>C] glucose revealed only 20% labeling (Fig 1B and C). The large majority of TCA carbons in ECs are therefore derived from glutamine. Neither the presence or absence of VEGF or other growth factors in the media, nor conditions of hypoxia or acidosis, appeared to modulate this high level of incorporation of glutamine-derived carbons into the TCA cycle (Appendix Fig S1).

**Table 1. Consumption of glucose and glutamine and production of lactate and glutamate by endothelial cells.**

	nmol/10,000 cells/h
Glucose consumption	8.54 ± 0.14
Lactate production	14.85 ± 0.17
Glutamine consumption	2.32 ± 0.36
Glutamate production	0.23 ± 0.05
Glycolysis index	1.74 ± 0.04
Glutamine index	0.10 ± 0.02

HUVECs were cultured for 24 h, and glucose, lactate, glutamine, and glutamate levels were measured in the media. The consumption and secretion were normalized to the levels of no-cell containing media. Glycolytic index is defined as lactate production/glucose consumption. Glutamine index is defined as glutamate production/glutamine consumption. Data shown as mean ± SD, *n* = 3.

The carboxylation of aKG to citrate (reductive carboxylation) has been reported in numerous tumor cells (Ward *et al*, 2010; Metallo *et al*, 2011; Mullen *et al*, 2011; Wise *et al*, 2011), but never studied in ECs. We took three approaches to estimate reverse carboxylation in ECs. (i) When the TCA cycle proceeds in the usual forward direction, citrate that is derived from [U-<sup>13</sup>C] glutamine is labeled on four carbons (M4), whereas citrate is labeled on five carbons (M5) when reductive carboxylation occurs (Fig 2A). Nearly 8% of citrate in HUVECs bear five labeled carbons, while 62% of aKG was similarly labeled, indicating that ~13% of citrate was derived via reductive carboxylation. (ii) Malate, aspartate, and fumarate derived from [U-<sup>13</sup>C] glutamine and forward cycling in the TCA are labeled on all four carbons (M4), whereas the same metabolites derived from reductive carboxylation are labeled on only three carbons (M3, Fig 2A). The M3/M4 ratio for all three of these metabolites was 10–16% (Fig 1), indicating again a roughly 13% contribution of reductive carboxylation. (iii) Fatty acid synthesis is required for membrane formation and thus for cellular growth. Synthesis occurs via incorporation of carbons from cytosolic acetyl-CoA into growing fatty acids. When citrate is generated by reductive carboxylation of [U-<sup>13</sup>C] aKG, both carbons of the consequent cytosolic are <sup>13</sup>C-labeled, while neither carbon is labeled when citrate is generated by condensation of oxaloacetate (Fig 2A). Incorporation of <sup>13</sup>C label from glutamine to fatty acids thus reflects active reductive carboxylation. Knock-down of ATP citrate lyase (ACLY) significantly reduced the incorporation of <sup>13</sup>C-labeled glutamine to fatty acids (Appendix Fig S2A), and led to growth arrest in the absence of exogenous fatty acids (Appendix Fig S2B), indicating that glutamine-derived carbon incorporation into fatty acids via ACLY-mediated conversion of cytosolic citrate to acetyl-CoA is critical for cell growth. [U-<sup>13</sup>C] glutamine contributed about 10% as many carbons to fatty acid synthesis as did [U-<sup>13</sup>C] glucose (Fig 2A). The much higher contribution of glucose to fatty acid synthesis suggests that most 2-carbon units derive from glucose, and is consistent with the high 2-carbon labeling of citrate in the presence of [U-<sup>13</sup>C] glucose (Fig 1B). Together, these data indicate a roughly 10–13% rate of reverse carboxylation compared to the generation of citrate via condensation of oxaloacetate with acetyl-CoA, a rate comparable to various tumor cells (Metallo *et al*, 2011; Mullen *et al*, 2011; Wise *et al*, 2011).

Malic enzyme decarboxylates malate to pyruvate, which can then again be decarboxylated to acetyl-CoA by pyruvate dehydrogenase (Fig 2B), in the process generating NADPH that can be used in the synthesis of fatty acids. In the presence of [U-<sup>13</sup>C] glutamine, citrate that is labeled on all six carbons thus indicates that oxaloacetate condensed with acetyl-CoA that was derived from glutamine via malic enzyme. 2% of citrate in HUVECs grown in the presence of [U-<sup>13</sup>C] glutamine was labeled on all six carbons, compared to 38% labeling on four carbons, indicating that ~8–9% of carbons flowing through pyruvate dehydrogenase were derived from glutamine. Lastly, we observed > 50% labeling by [U-<sup>13</sup>C] glutamine of proline, aspartate, asparagine, and glutamate, all of which are non-essential amino acids derived from glutamine (Fig 2C). Together, these data demonstrate that ECs use a large portion of carbons derive from glutamine for synthesis of biomass.

In light of the high consumption of glutamine by ECs, we next tested whether glutamine was required for various critical endothelial functions, including viability, proliferation, and migration,

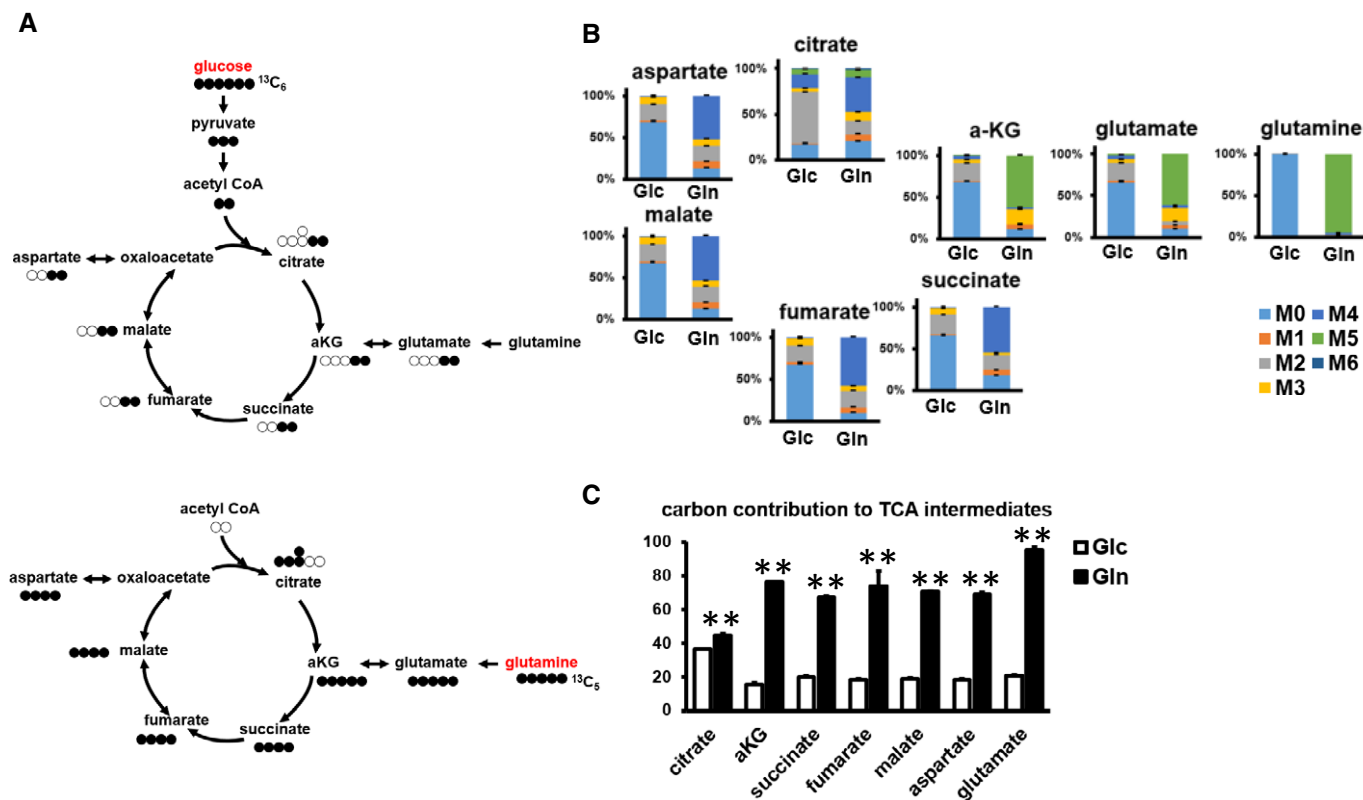


**Figure 1. Glutamine and glucose contribution to TCA metabolism in ECs.**

**A** Schematic of labeling scheme, using either [U- $^{13}\text{C}$ ] glucose or [U- $^{13}\text{C}$ ] glutamine. For simplicity, labeling of only the first round in TCA cycle is shown.

**B** HUVECs were cultured for 24 h in the presence of tracer (either [U- $^{13}\text{C}$ ] glucose (Glc) and  $^{12}\text{C}$  glutamine (Gln) or  $^{12}\text{C}$  Glc and [U- $^{13}\text{C}$ ] Gln), followed by mass spectrometry of the indicated metabolites. The color codes indicate the % of each metabolite that is heavy isotope-labeled by the indicated number of carbons. M+n: a metabolite with  $n$  carbon atoms labeled with  $^{13}\text{C}$ .

**C** Total percentage of carbons, for each TCA metabolite, that is heavy isotope-labeled in the presence of [U- $^{13}\text{C}$ ] Glc or [U- $^{13}\text{C}$ ] Gln. Approximately 70% of carbons in the TCA cycle derive from glutamine, while less than 20% of carbons derive from glucose.

Data information: Glc: glucose; Gln: glutamine. Data shown as mean  $\pm$  SD,  $n = 3$ . Glc versus Gln,  $**P < 0.01$ .  $P$ -values were calculated by using two-tailed Student's  $t$ -test.

hallmarks of angiogenesis. HUVECs cultured in media with diminishing concentrations of glutamine revealed that endothelial proliferation requires glutamine consumption in a concentration-dependent manner (Fig 3A). In addition, HUVECs cultured in glutamine-deficient medium for 4 days displayed a significant activation of apoptosis, as determined by Annexin V staining (Fig 3B). GLS catalyzes the de-amination of glutamine to glutamate and is the initial step in glutamine catabolism. GLS1 is the main isoform of GLS expressed in ECs (Appendix Fig S3A; Consortium, 2015). GLS1 in ECs is localized in mitochondria (Fig 3C), as in other cells (Klingman & Handler, 1958; Masson *et al.*, 2006). GLS1 knockdown by siRNA (Appendix Fig S3B and C) markedly reduced endothelial growth (Fig 3C and Appendix Fig S3D), approximating that seen in 0.1 mM glutamine (Fig 3A). Similarly, the GLS-specific inhibitor bis-2-(5-phenylacetamido-1,3,4-thiadiazol-2-yl) ethyl sulfide (BPTES) also inhibited endothelial proliferation in a dose-dependent manner (Fig 3D). In addition, in an *ex vivo* analysis of angiogenesis that requires active proliferation (Appendix Fig S4), aortic explants from wild-type mice revealed markedly impaired capillary sprouting when glutamine was removed from the medium (Fig 3E). Together, these observations indicate ECs depend critically on a supply of extracellular glutamine for proliferation, and ultimately for viability.

We next tested whether ECs require glutamine for cellular migration, another critical hallmark of angiogenesis. Surprisingly, despite the pronounced effect on proliferation, ECs retained full capacity for migration in the absence of glutamine, as determined in transwell assays (Fig 4A) or scratch assays (Appendix Fig S5A). Genetic inhibition of GLS1 by siRNA, or pharmacological inhibition with BPTES, similarly had no impact on cellular migration by ECs (Fig 4B and C, respectively, and Appendix Fig S5B). On the other hand, deprivation of glucose profoundly blocked migration (Fig 4A). These observations suggest that EC migration relies largely on glycolysis, and not on oxidative phosphorylation. Consistent with this notion, neither pharmacological inhibition of complexes I and II of the electron transport chain, nor inhibition of the mitochondrial ATPase, had any appreciable impact on EC migration despite significant suppression of EC proliferation (Appendix Fig S6). These data demonstrate a fundamental difference in how ECs use glucose and glutamine for different cellular processes.

To test the role of glutamine in EC biology *in vivo*, we generated mice that lack GLS1 specifically in ECs, using mice bearing floxed alleles of GLS1 (Mingote *et al.*, 2015) and a transgene encoding for tamoxifen-activated Cre recombinase driven by the EC-specific V-cadherin promoter (Monvoisin *et al.*, 2006). Following tamoxifen

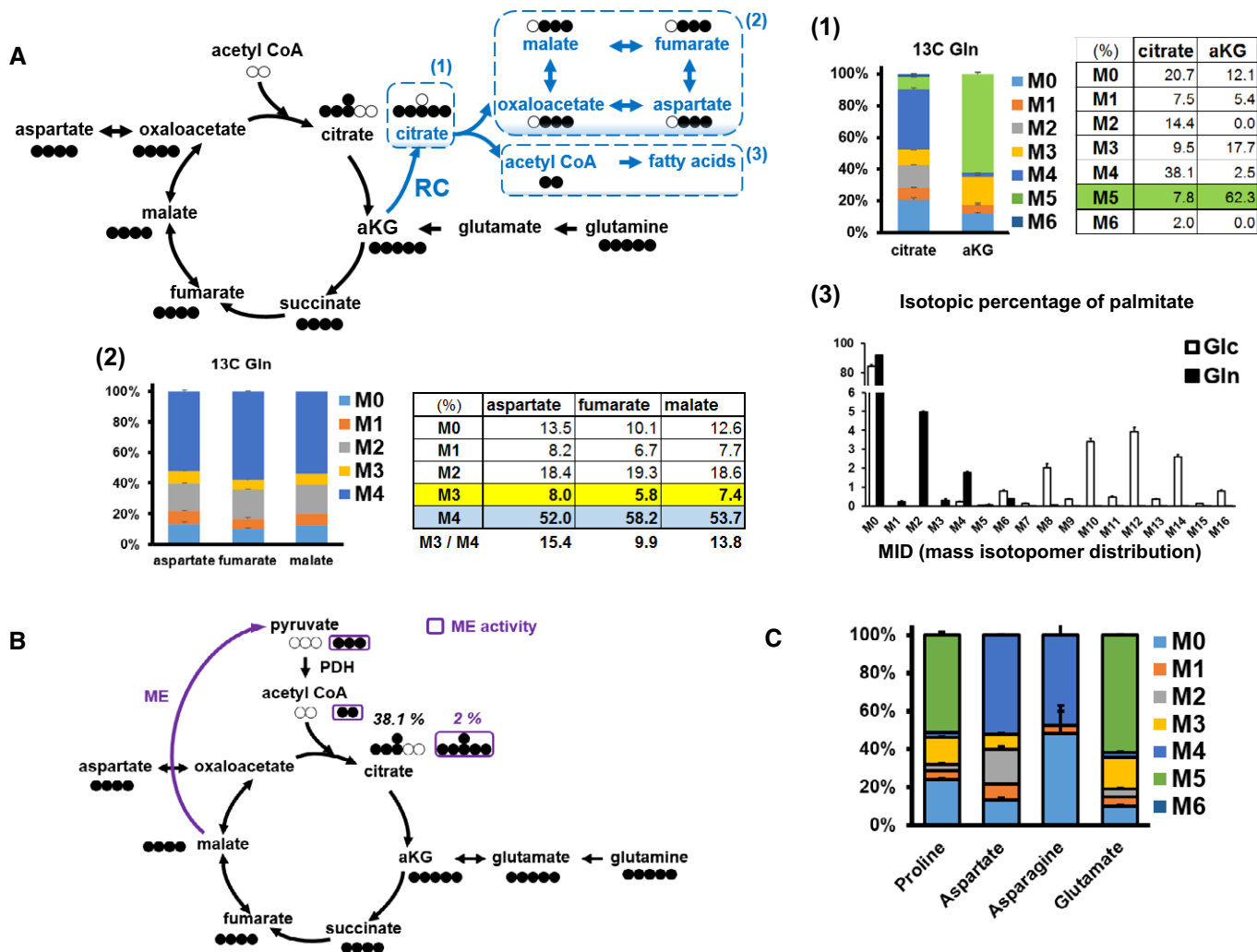


**Figure 2. Glutamine and cataplerosis in endothelial cells.**

A Schematic depicting three approaches to estimate reductive glutamine metabolism with [U-<sup>13</sup>C] glutamine. (1) Ratio of M+5 citrate to M+5 aKG indicates the portion of citrate that is derived from aKG (12.5%). (2) Ratio of M+3 to M+4 4-carbon members of TCA cycle indicates the portion that are derived from oxidation versus reduction in aKG (15.4% for aspartate, 9.9% for fumarate, and 13.8% for malate). (3) Ratio of labeled FA carbons from [U-<sup>13</sup>C] Glc versus [U-<sup>13</sup>C] Gln reflects the portion of citrate that is derived from aKG versus condensation with glucose-derived Ac-CoA.

B Schematic depicting estimation of malic enzyme (ME) flux from [U-<sup>13</sup>C] Gln. The ratio of M+6 to M+4 citrate suggests ME activity.

C Labeling of non-essential amino acids (proline, aspartate, asparagine, and glutamate) from [U-<sup>13</sup>C] Gln.

Data information: Glc: glucose; Gln: glutamine. Data shown as mean ± SD, n = 3.

administration from postnatal day (P)1 to P3, GLS1 mRNA and protein expression was efficiently suppressed (Appendix Fig S7A and B). Subsequent analysis of retinal vasculature at P5 revealed marked reduction in vessel density in both angiogenic front and rear plexus in mice lacking EC GLS (GLS<sup>ΔEC</sup>) compared to control mice (Fig 5A, C and E), but no change in large vessels (Fig 5B). EC proliferation was significantly blunted in GLS<sup>ΔEC</sup> mice, as evidenced by pH3 staining (Fig 5C), leading to a strong reduction in the total number of ECs (Fig 5D). In contrast, analysis of the tip cells revealed no impact on the number of tip cells and filopodia in GLS<sup>ΔEC</sup> mice (Fig 5F and G), consistent with the cell culture experiments indicating that glutamine metabolism is not required for EC migration. In addition, capillary sprouting from aortic rings derived from GLS<sup>ΔEC</sup> mice was significantly impaired, compared to controls (Fig 5H), and the proliferation of isolated ECs was significantly blunted

(Appendix Fig S7C). Glutamine consumption is thus required for EC proliferation and angiogenesis *in vivo*. Of note, compensatory mechanisms clearly exist *in vivo*, as GLS<sup>ΔEC</sup> mice did develop to adulthood, and appeared grossly normal (Appendix Fig S7D and E).

Together, the above data demonstrate the critical role that glutamine plays in EC proliferation and angiogenesis, both in cell culture and *in vivo*. To probe the mechanism of glutamine requirement, and in light of the strong contribution of glutamine to TCA intermediates (Fig 1), we next tested the levels of TCA intermediates in the absence of glutamine. As seen in Fig 6, the absence of glutamine led to near-total collapse of all TCA intermediates, while glycolysis intermediates were not altered. Genetic inhibition of GLS1 with siRNA phenocopied glutamine withdrawal, while levels of glutamine itself were increased, consistent with block of glutamine catabolism (Fig 6A). Defects in glutamine anaplerosis can in principle

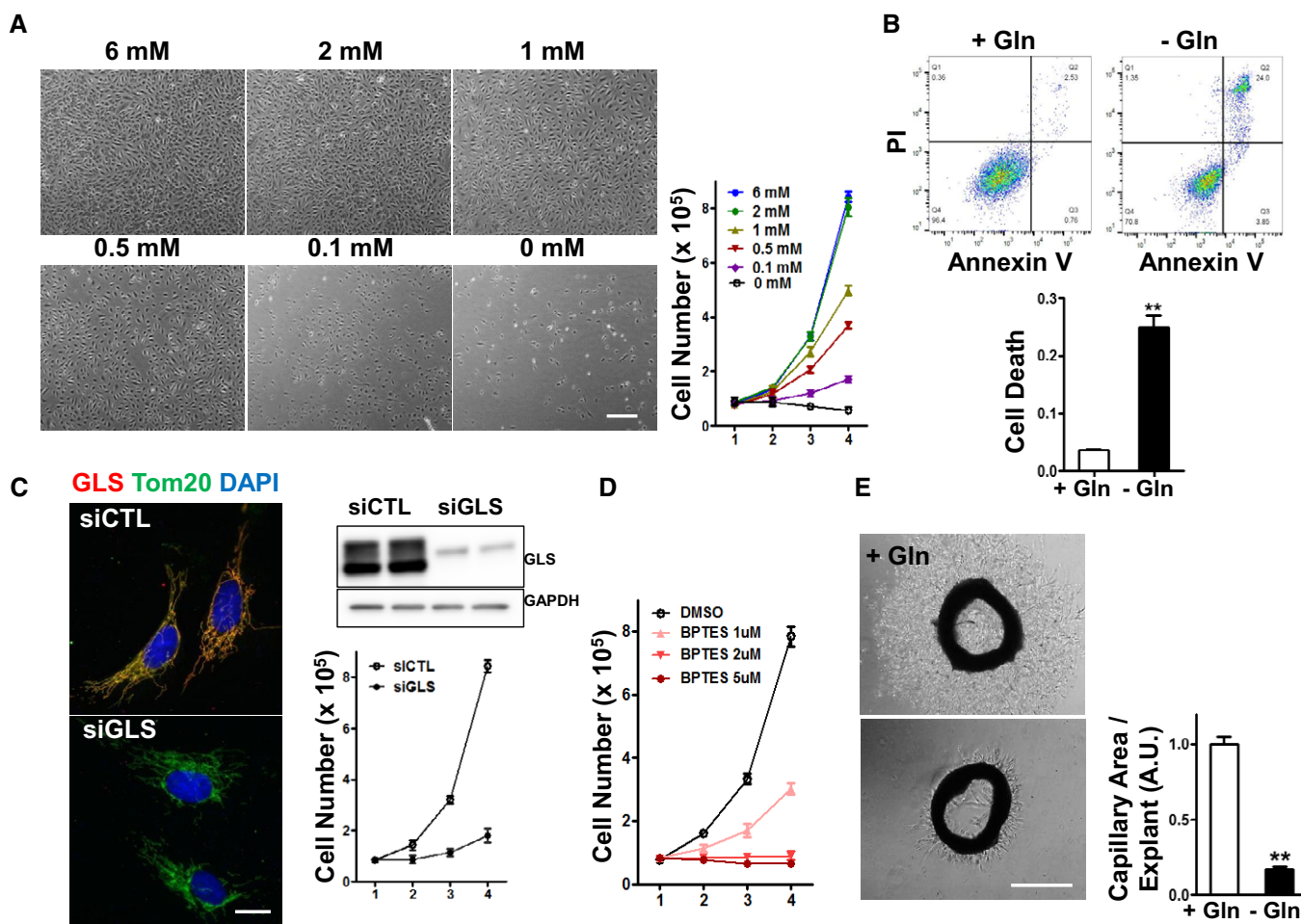


**Figure 3. Glutamine is required for EC proliferation and viability.**

**A** EC proliferation is dependent on glutamine. Growth curves (right) and phase contrast images (40 $\times$ , left) of HUVECs after 4 days of culture in medium with the indicated concentrations of glutamine. Scale bar = 100  $\mu$ m.

**B** Glutamine depletion induces apoptotic cell death, assessed by Annexin V and PI staining 4 days after glutamine (Gln) depletion.

**C** GLS is located in the mitochondria, and knockdown of GLS impairs EC proliferation. Immunofluorescence (400 $\times$ , left) for GLS (red), Tom20 (green) and DAPI (blue), and immunoblotting (top right) for GLS and GAPDH at day 4 of culture. Growth curve (bottom right) of HUVECs transfected with siRNA against GLS and control (CTL) in glutamine-containing medium. Scale bar = 10  $\mu$ m.

**D** Growth curve of HUVECs treated with the indicated doses of selective GLS inhibitor BPTES. For all proliferation assay, cells are counted by TC20<sup>TM</sup> Automated Cell Counter.

**E** Glutamine depletion impairs capillary sprouting from mouse aortic explants. At day 3 of aortic ring explant incubation, each explant was photographed and the area of capillary outgrowth was quantified using ImageJ. Scale bar = 1 mm.

Data information: Data are represented as mean  $\pm$  SEM,  $n = 3$  (A–D) or  $n > 4$  segments per aorta from three mice each (E). +Gln versus –Gln, \*\* $P < 0.01$ .  $P$ -values were calculated by using two-tailed Student's  $t$ -test.

be compensated by anaplerosis from glucose, via pyruvate carboxylase (PC)-mediated carboxylation of pyruvate to oxaloacetate (Fig 6B). Surprisingly, however, tracing experiments using [U-<sup>13</sup>C] glucose revealed no compensation by PC, as determined by levels of M+3 fumarate, step-increase in the M+3/M+2 ratio from succinate to fumarate, or appearance of M+5 citrate. Relative contribution from glucose oxidation via PDH flux, indicated as M+2 labeled TCA intermediates, was also not induced and rather reduced in the presence of siGLS. These data demonstrate the fundamental reliance of ECs on glutamine as a source of anaplerotic carbons. Consistent with loss of carbon sources, NTP synthesis was blunted in the absence of glutamine, as measure by C13-glucose incorporation (Appendix Fig S8A). Glutamine deprivation and siGLS also

reduced the energy charge of the cell (ATP/ADP ratio) by 50% (Appendix Fig S8B).

To test the role of anaplerosis in EC proliferation, we next tested whether replenishment of TCA intermediates can rescue proliferation. Supplementation with dimethyl  $\alpha$ -ketoglutarate (aKG), a cell-permeable form of aKG, significantly replenished TCA cycle intermediates in glutamine-depleted condition (Fig 7A). Strikingly, aKG supplementation also significantly rescued cell proliferation of ECs in glutamine-depleted medium (Fig 7B) or cells treated with siGLS (Fig 7C). Moreover, aKG supplementation also completely reversed the increase in apoptosis noted in the absence of glutamine (Fig 7D). We conclude that anaplerosis of TCA is a critical component of EC viability and proliferation.

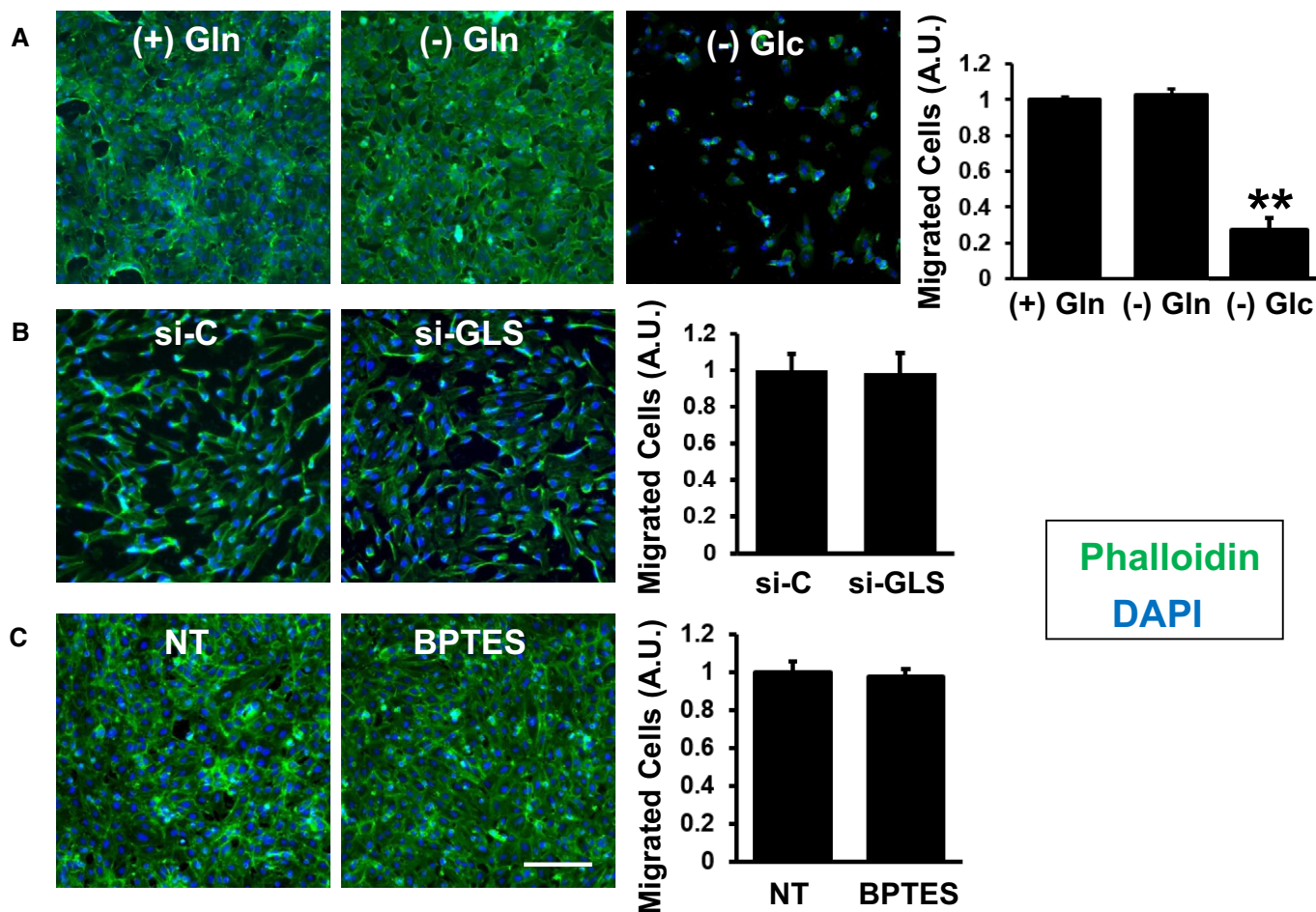


**Figure 4. Glutamine is not required for EC migration.**

A–C Migration of HUVECs was quantified in the presence or absence of glutamine (Gln) or glucose (Glc) (A), or treated with si-control (C) versus si-GLS (B), or treated with BPTES versus no treatment (NT) (C). The same number of cells was seeded into the upper chamber of transwell plates and allowed to migrate for 12 h. Cells that migrated across the transwell membrane were visualized by staining with phalloidin (green) and DAPI (blue). Glc: glucose; Gln: glutamine. Scale bar = 100  $\mu$ m. Data shown as mean  $\pm$  SD,  $n = 6$ . (+)Gln versus (–)Glc,  $**P < 0.01$ .  $P$ -values were calculated by using two-tailed Student's  $t$ -test.

Glutamine contains two nitrogens per molecule, whereas aKG contains none. The rescue of EC proliferation by aKG in the absence of glutamine (Fig 7) thus raised a conundrum: Where do the cells acquire the nitrogens needed for biomass synthesis? Some nitrogens can be acquired from transamination of nitrogens in the alpha position of imported essential amino acids provided in the media. However, a number of processes require

specifically the distal amide nitrogen from glutamine. For example, the amide nitrogen of glutamine is required for the biosynthetic generation of asparagine (Appendix Fig S9A), as demonstrated in ECs by incorporation of label into asparagine from glutamine with  $^{15}\text{N}$ -labeled at the amide position (Appendix Fig S9B). One explanation for the conundrum may be that, in the absence of glutamine, ECs synthesize glutamine, in

**Figure 5. Glutaminolysis is required for angiogenesis *in vivo*.**

A–G Staining of WT versus GLS<sup>AEC</sup> mouse retina at postnatal day (P)7. Tamoxifen was injected for three consecutive days from P1 to P3, and retinal vasculature was analyzed at P7. (A) The entire retinal vasculature is visualized by IB4 staining. Scale bar = 1 mm. (B) Arteriovenous (a/v) patterning was analyzed by IB4 and SMA staining (C–E). Vascular density (angiogenic front: C and rear plexus: E), number of branching points, and number of pH3-positive cells were analyzed by either CD31, IB4, pH3, or ERG staining. Number of tip cells (F) and filopodia (G) are visualized via IB4 staining under high-power magnification. Quantifications are at bottom of figure and represent data from three independent experiments (mean  $\pm$  SD,  $n = 7$ –9, WT versus GLS<sup>AEC</sup>,  $**P < 0.01$ ). Magnification of objective lens (A: 2 $\times$ , B: 5 $\times$ , C and E: 10 $\times$ , D and F: 20 $\times$ , G: 63 $\times$ ). Scale bars = 50  $\mu$ m. White arrowheads indicate pH3-positive proliferating ECs, red triangles indicate tip cells, yellow dots indicate filopodia, red dotted lines indicate body of tip cells, and blue dotted lines indicate the boundary of tip cell and stalk cell.  $P$ -values were calculated by using two-tailed Student's  $t$ -test.

H Capillary sprouting of aortic explants from WT versus GLS<sup>AEC</sup> mouse. At day 3 of aortic ring explant incubation, each explant was photographed and the area of capillary outgrowth was quantified using ImageJ. Data are represented as mean  $\pm$  SD,  $n > 4$  segments per aorta from three mice each. WT versus GLS<sup>AEC</sup>,  $*P < 0.05$ .  $P$ -values were calculated by using two-tailed Student's  $t$ -test.

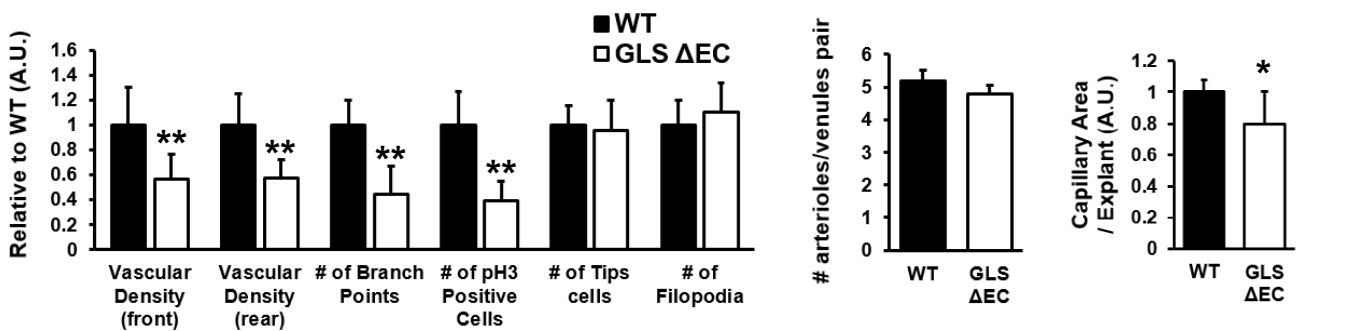
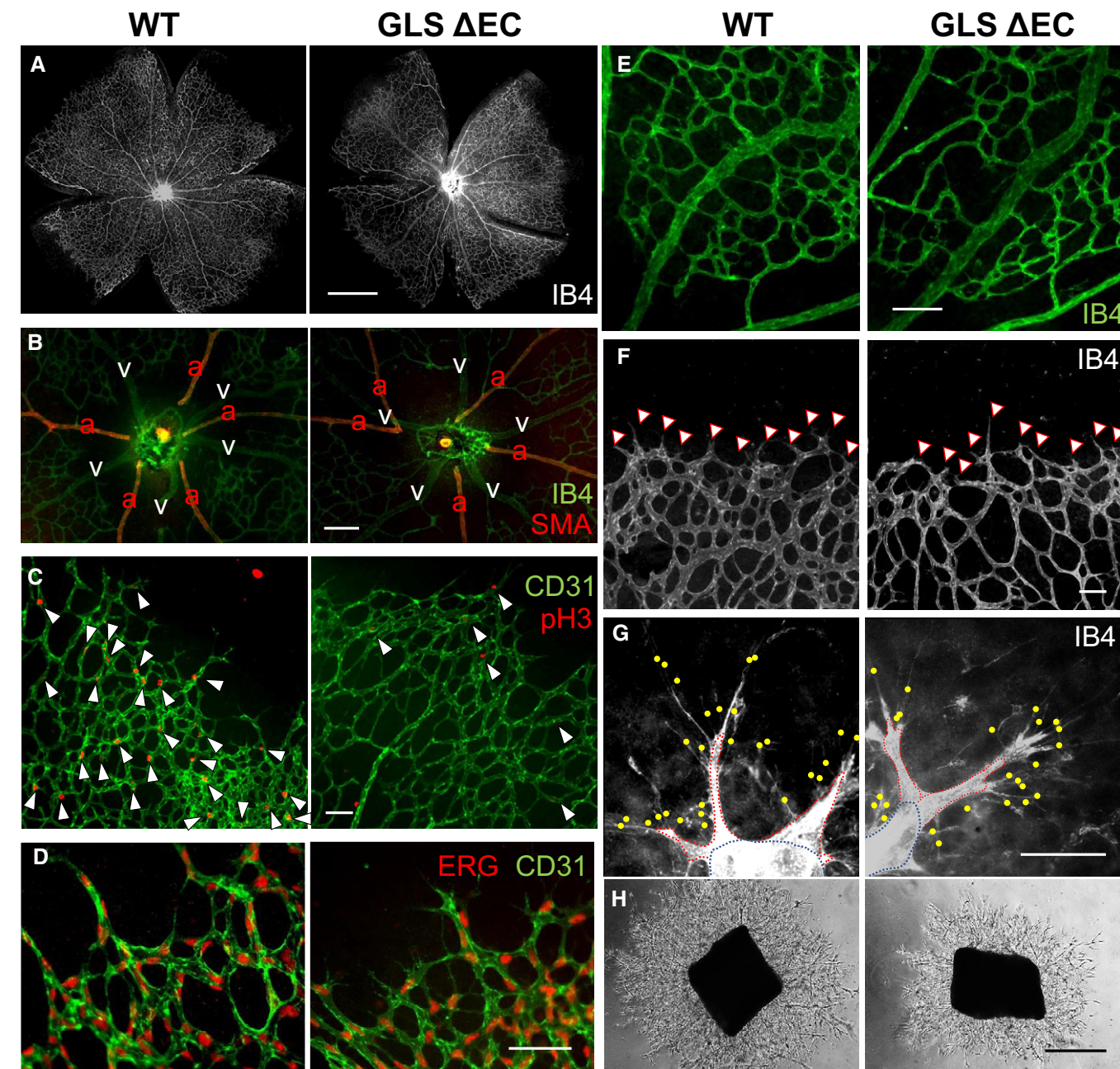
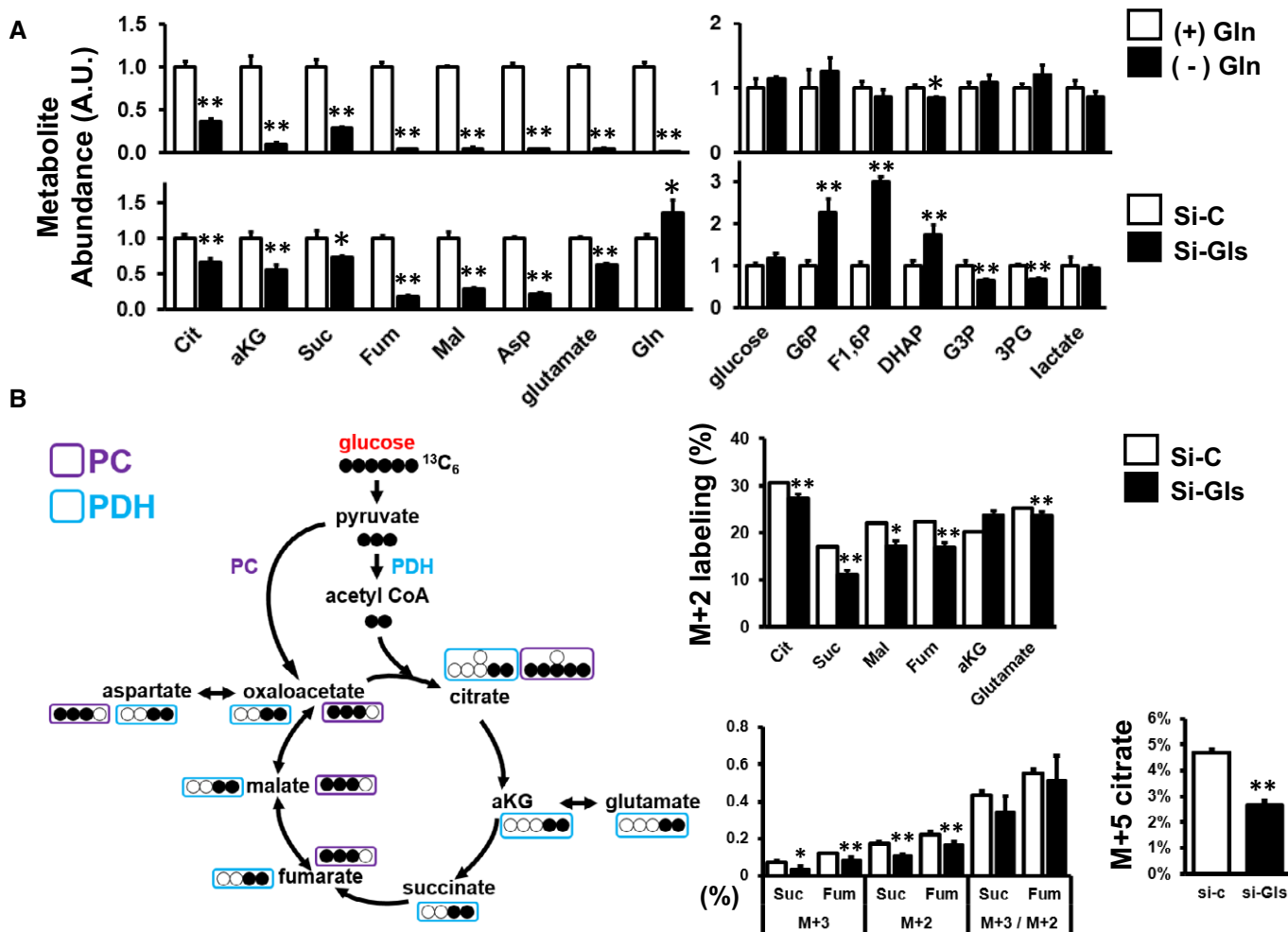


Figure 5.





**Figure 6. Collapse of TCA cycle intermediates in the absence of glutamine.**

**A** Relative abundance of TCA cycle and glycolysis metabolites. HUVECs were cultured with (+ Gln) or without (– Gln) glutamine (upper panel) or transfected with control or GLS siRNA (lower panel) and intracellular TCA cycle (left panel) and glycolysis (right panel) intermediates were quantified by mass spectrometry after 24 h of incubation.

**B** Absence of compensation by pyruvate dehydrogenase (PDH) or pyruvate carboxylase (PC). Left: Schematic depicting approach to estimate relative PC and PDH flux from [U- $^{13}C$ ] Glc. Right top: Relative PDH activity in si-control (C) versus si-Gls conditions, estimated by M+2 labeled of TCA intermediates. Right bottom: Relative PC activity identified by comparing the M+3/M+2 ratio of succinate to that of fumarate. Rightmost bottom: M+5 citrate as an additional measure of relative PC activity.

Data information: Cit: citrate, aKG: alpha-ketoglutarate, Suc: succinate, Fum: fumarate, Mal: malate, Asp: aspartate, Gln: glutamine, G6P: glucose 6-phosphate, F1,6P: fructose 1-6-bisphosphate, DHAP: dihydroxyacetone phosphate, G3P: glycerol 3-phosphate, 3PG: 3-phosphoglycerate. Data shown as mean  $\pm$  SD,  $n = 3$ . (+)Gln versus (–)Gln or si-C versus si-Gls: \*\* $P < 0.01$ ; \* $P < 0.05$ .  $P$ -values were calculated by using two-tailed Student's  $t$ -test.

order to provide amide nitrogen for asparagine synthesis. However, even with aKG supplementation, only marginal intracellular glutamine levels were observed in the absence of extracellular glutamine (Appendix Fig S9C).

Other sources of extracellular nitrogen and/or asparagine therefore likely exist. One such source could be the import of extracellular proteins, via the macropinocytosis pathway, followed by lysosome-mediated protein breakdown. Consistent with this notion, we noted dramatically increased import of labeled macromolecules (Texas Red-Dextran) in cells growing in the presence of aKG but absence of glutamine (Fig 8A). The process was inhibited by amiloride, an inhibitor of macropinocytosis (Fig 8A). Macropinocytosis is thus strongly induced by glutamine withdrawal in ECs. Supporting the notion that protein import supports cell proliferation,

the addition of 3% BSA to the medium accelerated cellular growth (Fig 8B). To formally test whether the activation of pinocytosis was required for cellular growth, we treated cells with amiloride and monitored their growth. Treating cells growing in complete media with amiloride had little impact (not shown), but treating cells growing in the absence of glutamine and presence of aKG led to complete growth arrest, and accelerated cell death (Fig 8C). Supplementation of the amiloride-treated cells with non-essential amino acids (NEAAs), including asparagine, rescued both loss of viability and proliferation arrest caused by amiloride (Fig 8C). Similar inhibition of proliferation and rescue by NEAAs were observed with genetic inhibition of macropinocytosis via siRNA directed against Rac1, a crucial component of macropinocytosis (Fig 8D; Fujii *et al*, 2013), or with pharmacologic inhibition with EIPA, another

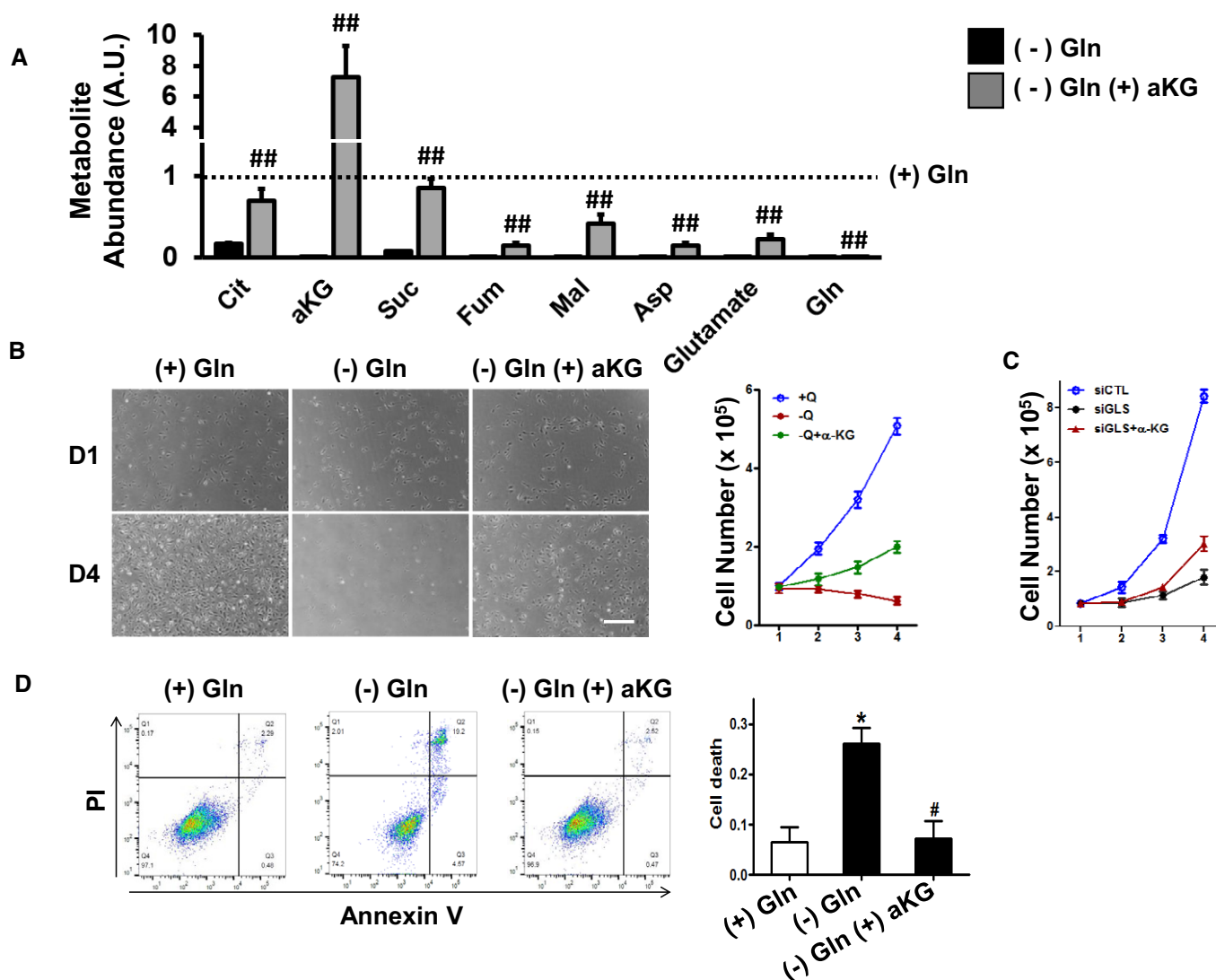


**Figure 7. Extracellular aKG restores TCA cycle intermediates and rescues EC proliferation and viability in the absence of glutamine.**

**A** aKG supplementation restores intracellular TCA cycle intermediates in glutamine-depleted conditions. Cell-permeable aKG (7 mM) was added to glutamine-depleted media, and the abundance of TCA cycle intermediates was measured by mass spectrometry. Values are indicated as relative to (+)Gln condition (dotted line).

**B** aKG supplementation rescues proliferation in glutamine-depleted condition. Growth curve and phase contrast images (40 $\times$ ) of HUVECs during 4 days of culture in (+)Gln, (-)Gln, and (-)Gln (+)aKG condition. Scale bar = 100  $\mu$ m.

**C** aKG supplementation similarly rescues proliferation in si-Glns condition.

**D** aKG supplementation rescues viability in glutamine-depleted condition. Cell death was assessed by Annexin V and PI staining after 4 days of culture in the indicated condition.

Data information: Data are represented as mean  $\pm$  SEM,  $n = 3$ . In (A): (-)Gln versus (-)Gln (+)aKG,  $^{##}P < 0.01$ . In (D):  $^{*}P < 0.05$  versus (+)Gln,  $^{#}P < 0.05$  versus (-)Gln.  $P$ -values were calculated by using two-tailed Student's  $t$ -test (A) or one-way ANOVA followed by Bonferroni *post hoc* test (D).

inhibitor of macropinocytosis, and rescue with asparagine alone (Appendix Fig S9D). We conclude that macropinocytosis is activated in the absence of glutamine and is critically required for the import of nitrogen sources needed for cellular proliferation.

## Discussion

We show here that ECs consume significant amounts of glutamine, that the majority of TCA carbons and nitrogens of some NEAA in ECs derive from imported glutamine, and that blocking glutamine

consumption metabolically, pharmacologically, or genetically, causes a collapse of TCA cycle intermediates that leads to proliferation arrest. Work by Huang *et al.*, reported in a manuscript also published in this issue, similarly demonstrates the essential nature of glutamine contribution to both TCA carbons and NEAA nitrogens, in particular to asparagine (Huang *et al.*, 2017), strongly supporting our findings.

Our data demonstrate that the metabolic demands of migration and proliferation in ECs differ fundamentally. Whereas glutamine carbons are absolutely required for proliferation, neither glutamine nor oxidative phosphorylation is required for EC migration. In stark

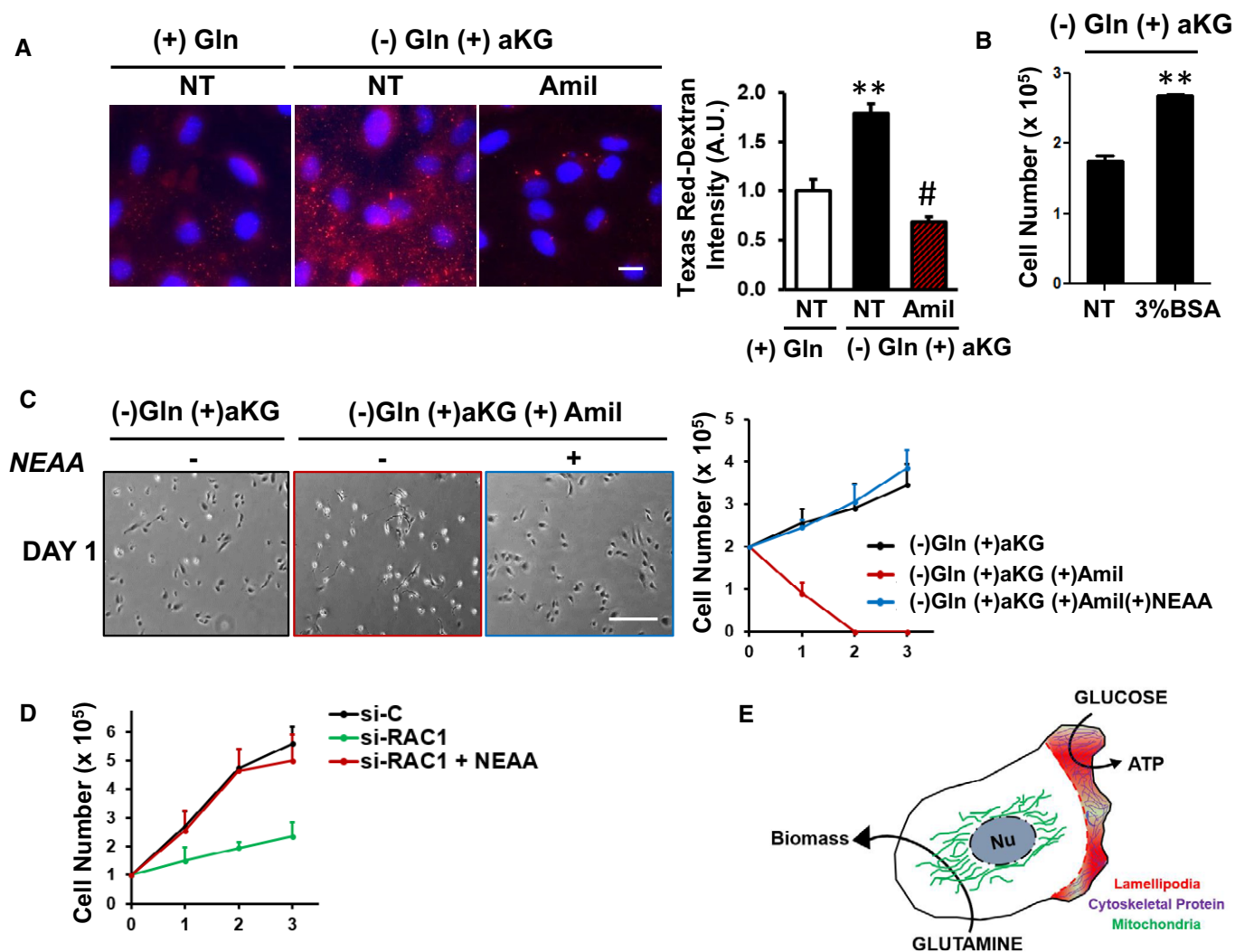


**Figure 8. Macropinocytosis is required for proliferation in the absence of glutamine.**

A Macropinocytosis is increased in the absence of glutamine. HUVECs were cultured in the presence and absence of glutamine with or without aKG or Amil (amiloride), and macropinocytosis was measured by Texas Red-Dextran uptake assay. Representative images are shown on the left, and quantification on the right. NT: no treatment. Scale bar = 10  $\mu$ m.  
 B Addition of 3% BSA promotes cell growth in glutamine-depleted and aKG-supplemented condition. HUVECs were cultured in the glutamine-depleted and aKG-supplemented medium with or without 3% BSA for 4 days.  
 C, D Macropinocytosis is necessary for EC survival and nitrogen source in glutamine-depleted and aKG-supplemented condition. (C) Left: HUVECs die upon amiloride (+ Amil) treatment, and viability is rescued by supplementation of non-essential amino acids (NEAA, 0.2 mM). Right: Growth curves of HUVECs under the same three conditions. Scale bar = 100  $\mu$ m. (D) Growth curves of HUVECs treated with si-RAC1 versus si-Control and si-RAC1 rescued with NEAA, as in (C).  
 E Schematic of compartmental use of glucose for ATP generation versus glutamine for generation of biomass (see text for details).

Data information: Data are represented as mean  $\pm$  SEM,  $n = 3$ . In (A): (+)Gln versus (-)Gln (+)aKG:  $^{***}P < 0.01$ ; (-)Gln (+)aKG versus (-)Gln (+)aKG (+)Amil:  $^{#}P < 0.05$ . In (B):  $^{**}P < 0.01$ .  $P$ -values were calculated by using two-tailed Student's  $t$ -test (B) or one-way ANOVA followed by Bonferroni *post hoc* test (A).

contrast, glucose is absolutely required for EC migration. One possibility for this striking difference is that glycolysis is used in large part to generate ATP, and less so for biosynthetic processes, while the opposite is true for glutamine. This conclusion is consistent with the observations that (i) > 90% of glucose-derived carbons are secreted from the cell in the form of lactate, that is not contributing to biomass, while 90% of glutamine-derived carbons are incorporated into TCA intermediates and consequent cellular building blocks; and (ii) conversely, removal of glutamine or inhibition of GLS led to pronounced reductions in TCA intermediates. In

migrating ECs, glycolytic enzymes can be found in actin-associated multi-enzyme complexes, known as metabolons, located largely in sites of high ATP need adjacent to lamellipodia and filopodia driving the migratory phenotype (De Bock *et al*, 2013; Jang & Arany, 2013). In contrast, glutamine-consuming enzymes are found largely in mitochondria, located largely perinuclear and far from the primary need for ATP. We thus suggest that, in ECs, there is compartmentalization of glucose and glutamine consumption, the former serving to generate ATP at the migratory edge, the latter serving to generate biosynthetic precursors within mitochondria (Fig 8E).

Our results also reveal a critical requirement in ECs for macropinocytosis when extracellular glutamine is limiting but alternate sources of carbons are available. Macropinocytosis appears largely to serve the function of providing nitrogen groups, and not carbons, because (i) macropinocytosis does not rescue EC proliferation when alternate sources of carbons are not available, and (ii) the addition of non-essential amino acids rescues inhibition of macropinocytosis. Understanding how mechanistically macropinocytosis is activated in the absence of glutamine will be of interest, and may involve relieving inhibition by the mTOR pathway (Palm *et al*, 2015).

The absence of compensatory anaplerosis from glucose, in the absence of glutamine or glutaminolysis, is interesting. Pyruvate carboxylase (PC) can normally contribute to the generation of oxaloacetate, and in the near-absence of oxaloacetate PC would be expected to be activated. The absence of PC activity may reflect the compartmentalization discussed above (Fig 8E): Pyruvate is generated near the plasma membrane by localized glycolysis and may thus not be readily available in sufficient quantities in the mitochondrial matrix. This compartmentalization would be consistent with the low levels of flux observed across the pyruvate dehydrogenase complex at baseline, and even lower when glutamine consumption is suppressed.

The less dramatic phenotype of GLS deletion *in vivo* than in cell culture likely reflects existing compensatory mechanisms in intact animals, as is often the case. For example, other sources of carbons may be available *in vivo*, akin to aKG, which in combination with activation of pinocytosis, may suffice to significantly rescue proliferation. Alternatively, it is also possible that ECs *in vivo* use less glutamine than in cell culture, as has been suggested for tumor cells (Mayers & Vander Heiden, 2015).

Tumor growth depends on nutrient supply, and thus on angiogenesis (Folkman, 1971; Weis & Cheresh, 2011). However, clinical efforts at suppressing tumor angiogenesis with anti-growth factor therapy have met with mixed success in the clinic (Bergers & Hanahan, 2008; Sennino & McDonald, 2012), indicating the need for new approaches. There are ongoing clinical efforts to develop glutaminase inhibitors as anticancer agents. These efforts were initially motivated by the key role of glutamine as an anaplerotic substrate in cancer cells. Our findings raise the possibility that glutaminase inhibition, perhaps in combination with other agents, could have benefits in cancer also through impairing angiogenesis.

## Materials and Methods

### Culture of human endothelial cells

Pooled human umbilical vein endothelial cells (HUVECs) were purchased from Lonza and used between passages 3 and 5. Cells were grown in EBM-containing EGM supplements (Lonza, CC-3121 & CC-4133) with 10% FBS. For glutamine deprivation experiments, DMEM was used with supplementation of EGM bullet kit (Lonza, CC4133), 5 mM glucose, 10% dialyzed FBS (HyClone), and penicillin/streptomycin. Glutamine, aKG, and/or NEAA were supplemented at indicated concentrations. For siRNA transfection, control siRNA (SIC001), and GLS siRNA mix (target sequences are CCUGAAGCAGUUCGAAAUA, CUGAAUAUGUGCAUCGAUA, AGAAAGUGGAGAUUCGAAAUA, and

GCACAGACAUGGUUGGUAU; all from Sigma-Aldrich) were used. The knockdown efficiency of each GLS siRNA and their effect on EC proliferation was verified (Appendix Fig S3C and D).

### Cell viability assay

Cell viability was assessed using the Dead Cell Apoptosis Kit with Annexin V Alexa Fluor<sup>®</sup> 488 & Propidium Iodide (PI; Thermo Fisher) kit according to manufacturer's instructions and analyzed via flow cytometry.

### Extracellular metabolic measurements

Glucose and glutamine consumption and lactate and glutamate production were measured by using a YSI 7100 Bioanalyzer. Media were collected after 24-h incubation in growing HUVECs and spin-down to remove cell debris. Collected supernatant was used for measurements, and values are normalized to cell number area under the curve as previously described (Lee *et al*, 2014).

### Mice

All mouse experiments were performed according to procedures approved by the University of Pennsylvania Institute for Animal Care and User Committees. Previously described *Gls1<sup>lox/lox</sup>* mice (Mingote *et al*, 2015) were maintained on mixed 129SvEv × C57BL/6J background. Endothelial cell-specific loss-of-function of GLS (GLS<sup>ΔEC</sup>) mice were generated by breeding *Gls1<sup>lox/lox</sup>* mice with transgenic mice expressing Cre recombinase under the tamoxifen-inducible VE-cadherin promoter (Monvoisin *et al*, 2006; kindly provided by Dr. Ralf Adams).

### Retina staining

To analyze blood vessel growth in the postnatal retina, tamoxifen (50ug) was injected into each pup from P1 to P3. On P5, whole mouse eyes were isolated and fixed in 4% PFA on ice for 10 min. Eyes were washed in PBS before the retinas were dissected and partially cut into four leaflets. After blocking/permeabilization in 5% BSA and 0.3% Triton X-100 (in PBS) for 1 h at room temperature, the retinas were incubated with primary antibody at 4°C overnight. Primary antibodies against the following proteins were used: Isolectin IB4 Alexa Fluor<sup>®</sup> 488 Conjugate (Thermo Fisher), CD31 (Millipore), ERG (Abcam). After washing in 0.3% Triton X-100, retinas were incubated with secondary antibodies at 4°C overnight. For IB4 staining, retina was mounted after washing without secondary antibody incubation.

### Transwell migration assay

ECs grown to subconfluence were detached by trypsinization, suspended in M199 media and applied to 8 μm pore transwell (10<sup>5</sup> cells/insert) precoated with gelatin, which was then inserted into a well containing EGM supplemented with 10% FBS. The cells were allowed to migrate across the membrane for 12 h. The cells that remained in upper chamber were removed by using cotton swab, and the migrated cells on the lower side of the membrane were stained with phalloidin and DAPI.

### Aortic capillary sprouting assay

Thoracic aorta segments (~500 µm long, > 6 segments per aorta) were dissected from two to three mice per group and implanted in matrigel as previously described (Baker *et al*, 2012). Each explant was photographed under microscope until day 3. The *ex vivo* angiogenesis was determined as the area of capillary outgrowth using ImageJ software.

### Isotopic labeling

The tracers [U-<sup>13</sup>C] glucose and [U-<sup>13</sup>C] glutamine were purchased from Cambridge Isotope Laboratories. Isotope-labeled glucose and glutamine medium was prepared in DMEM based media supplemented with EGM bullet kit as described above. Cells were cultured for 24 h in the presence of tracer, and metabolites were extracted by aspirating medium and immediately adding 80% methanol (MeOH) pre-chilled at 80°C. After 20 min of incubation on dry ice, the resulting mixture was scraped, collected into a centrifuge tube, and centrifuged at 10,000 × *g* for 5 min. Insoluble pellets were re-extracted with 1 ml of MeOH. The supernatants from two rounds of extraction were combined, dried under nitrogen gas, and analyzed by reversed-phase ion-pairing chromatography coupled with negative-mode ESI high-resolution MS on a stand-alone orbitrap (Xu *et al*, 2015).

### Fatty acids extraction

Cells were cultured in 10-cm dish for 3 days in the presence of tracer before extraction. 1 ml of 90% MeOH/0.3 M KOH was directly added to the cells and collected into a glass vial with a cap. The supernatant was heated at 80°C for 1 h for saponification and acidified by 100 µl of formic acid. Fatty acids were then subjected to two rounds of extraction with 1 ml hexane. The hexane from two rounds of extraction was combined, dried under nitrogen gas, re-suspended in 1 ml 1:1:0.3 chloroform/methanol/water and analyzed by reversed-phase ion-pairing chromatography coupled with negative-mode ESI high-resolution MS on a quadrupole time-of-flight (TOF) mass spectrometry.

### Macropinocytosis assay

HUVECs were serum-starved for 12 h. For a negative control, 1 mM of amiloride was treated in serum-free media for 30 min. After removing the medium from cells, cells were pulsed with Texas Red-Dextran (100 µg/ml; 70 kDa, lysine fixable) for 5 min. After removing the dextran containing medium, cells were washed with PBS and fixed with 4% paraformaldehyde in 250 mM HEPES for 30 min (Wang *et al*, 2014).

### Immunoblot analyses

Protein extraction and immunoblot analyses were performed using a RIPA lysis buffer (149 mM NaCl, 50 mM Tris pH 7.5, 0.1% sodium dodecyl sulfate, 1% Nonidet<sup>®</sup> P-40 Substitute, 0.5% deoxycholic acid, sodium salt) in the presence of protease and phosphatase inhibitors (Roche). Lysates were separated by SDS-PAGE under reducing conditions, transferred to a PVDF membrane,

and analyzed by immunoblotting. Primary antibodies used were rabbit anti-GLS (Abcam, ab156876 or Aviva System Biology, ARP55098 P050) and rabbit anti-GAPDH (Millipore). Appropriate secondary antibodies were from Cell Signaling Technology. Signal was detected using the ECL system (ImageQuant LAS 4000, Amersham Biosciences, GE Healthcare, Diegem, Belgium) according to the manufacturer's instructions.

### Statistics

*P*-values were calculated using the two-tailed Student's *t*-test. For statistical comparisons between study groups, one-way ANOVA was used, followed by Bonferroni *post hoc* testing. *P* < 0.05 was considered to be statistically significant. Data are displayed as mean ± SD or standard error (as indicated). All cell culture experiments included at least three biological replicates.

**Expanded View** for this article is available online.

### Acknowledgements

We thank Drs. Stephen Rayport and Chi Van Dang for contributing the GLS1 floxed mice, and Dr. Ralf Adams for the VCAD-ERTCre mice. This work was supported by grants from the National Institutes of Health (HL094499 and DK107667 to Z.A.), pilot funding and support from the DRC Regional Metabolomics Core (P30 DK19525), and an Established Investigator Award the American Heart Association (Z.A.).

### Author contributions

BK led the studies and was directly involved in most experiments. JL performed some cell culture, proliferation/apoptosis assays, and animal phenotyping. CJ conducted mass spectrometric analysis. ZA oversaw the studies. BK, JL, and ZA designed experiments, interpreted results, and wrote the manuscript. All authors discussed the results and commented on the manuscript.

### Conflict of interest

The authors declare that they have no conflict of interest.

## References

- Altman BJ, Stine ZE, Dang CV (2016) From Krebs to clinic: glutamine metabolism to cancer therapy. *Nat Rev Cancer* 16: 619–634
- Baker M, Robinson SD, Lechertier T, Barber PR, Tavora B, D'Amico G, Jones DT, Vojnovic B, Hodivala-Dilke K (2012) Use of the mouse aortic ring assay to study angiogenesis. *Nat Protoc* 7: 89–104
- Bergers G, Hanahan D (2008) Modes of resistance to anti-angiogenic therapy. *Nat Rev Cancer* 8: 592–603
- Consortium GT (2015) Human genomics. The Genotype-Tissue Expression (GTEx) pilot analysis: multitissue gene regulation in humans. *Science* 348: 648–660
- De Bock K, Georgiadou M, Schoors S, Kuchnio A, Wong BW, Cantelmo AR, Quaegebeur A, Ghesquiere B, Cauwenberghs S, Eelen G, Phng LK, Betz I, Tembuysen B, Brepoels K, Welti J, Geudens I, Segura I, Cruys B, Bifari F, Decimo I *et al* (2013) Role of PFKFB3-driven glycolysis in vessel sprouting. *Cell* 154: 651–663
- Eelen G, de Zeeuw P, Simons M, Carmeliet P (2015) Endothelial cell metabolism in normal and diseased vasculature. *Circ Res* 116: 1231–1244

- Folkman J (1971) Tumor angiogenesis: therapeutic implications. *N Engl J Med* 285: 1182–1186
- Fujii M, Kawai K, Egami Y, Araki N (2013) Dissecting the roles of Rac1 activation and deactivation in macropinocytosis using microscopic photo-manipulation. *Sci Rep* 3: 2385
- Hay N (2016) Reprogramming glucose metabolism in cancer: can it be exploited for cancer therapy? *Nat Rev Cancer* 16: 635–649
- Huang H, Vandekeere S, Kalucka J, Bierhansl L, Zecchin A, Brüning U, Visnagri A, Yuldasheva N, Goveia J, Cruys B, Brepoels K, Wyns S, Rayport S, Ghesquière B, Vinckier S, Schoonjans L, Cubbon R, Dewerchin M, Eelen G, Carmeliet P (2017) Role of glutamine and interlinked asparagine metabolism in vessel formation. *EMBO J* 36: 2334–2352
- Jang C, Arany Z (2013) Metabolism: sweet enticements to move. *Nature* 500: 409–411
- Klingman JD, Handler P (1958) Partial purification and properties of renal glutaminase. *J Biol Chem* 232: 369–380
- Lee JV, Carrer A, Shah S, Snyder NW, Wei S, Venneti S, Worth AJ, Yuan ZF, Lim HW, Liu S, Jackson E, Aiello NM, Haas NB, Rebbeck TR, Judkins A, Won KJ, Chodosh LA, Garcia BA, Stanger BZ, Feldman MD et al (2014) Akt-dependent metabolic reprogramming regulates tumor cell histone acetylation. *Cell Metab* 20: 306–319
- Leighton B, Curi R, Hussein A, Newsholme EA (1987) Maximum activities of some key enzymes of glycolysis, glutaminolysis, Krebs cycle and fatty acid utilization in bovine pulmonary endothelial cells. *FEBS Lett* 225: 93–96
- Li B, Qiu B, Lee DS, Walton ZE, Ochocki JD, Mathew LK, Mancuso A, Gade TP, Keith B, Nissim I, Simon MC (2014) Fructose-1,6-bisphosphatase opposes renal carcinoma progression. *Nature* 513: 251–255
- Masson J, Darmon M, Conjard A, Chuhma N, Ropert N, Thoby-Brisson M, Foutz AS, Parrot S, Miller GM, Jorisch R, Polan J, Hamon M, Hen R, Rayport S (2006) Mice lacking brain/kidney phosphate-activated glutaminase have impaired glutamatergic synaptic transmission, altered breathing, disorganized goal-directed behavior and die shortly after birth. *J Neurosci* 26: 4660–4671
- Mayers JR, Vander Heiden MG (2015) Famine versus feast: understanding the metabolism of tumors *in vivo*. *Trends Biochem Sci* 40: 130–140
- Metallo CM, Gameiro PA, Bell EL, Mattaini KR, Yang J, Hiller K, Jewell CM, Johnson ZR, Irvine DJ, Guarente L, Kelleher JK, Vander Heiden MG, Iliopoulos O, Stephanopoulos G (2011) Reductive glutamine metabolism by IDH1 mediates lipogenesis under hypoxia. *Nature* 481: 380–384
- Mingote S, Masson J, Gellman C, Thomsen GM, Lin CS, Merker RJ, Gaisler-Salomon I, Wang Y, Ernst R, Hen R, Rayport S (2015) Genetic pharmacotherapy as an early CNS drug development strategy: testing glutaminase inhibition for schizophrenia treatment in adult mice. *Front Syst Neurosci* 9: 165
- Monvoisin A, Alva JA, Hofmann JJ, Zovein AC, Lane TF, Iruela-Arispe ML (2006) VE-cadherin-CreERT2 transgenic mouse: a model for inducible recombination in the endothelium. *Dev Dyn* 235: 3413–3422
- Mullen AR, Wheaton WW, Jin ES, Chen PH, Sullivan LB, Cheng T, Yang Y, Linehan WM, Chandel NS, DeBerardinis RJ (2011) Reductive carboxylation supports growth in tumour cells with defective mitochondria. *Nature* 481: 385–388
- Palm W, Park Y, Wright K, Pavlova NN, Tuveson DA, Thompson CB (2015) The utilization of extracellular proteins as nutrients is suppressed by mTORC1. *Cell* 162: 259–270
- Sennino B, McDonald DM (2012) Controlling escape from angiogenesis inhibitors. *Nat Rev Cancer* 12: 699–709
- Vander Heiden MG, Cantley LC, Thompson CB (2009) Understanding the Warburg effect: the metabolic requirements of cell proliferation. *Science* 324: 1029–1033
- Verdegem D, Moens S, Stapor P, Carmeliet P (2014) Endothelial cell metabolism: parallels and divergences with cancer cell metabolism. *Cancer Metab* 2: 19
- Wang JT, Teasdale RD, Liebl D (2014) Macropinosome quantitation assay. *MethodsX* 1: 36–41
- Ward PS, Patel J, Wise DR, Abdel-Wahab O, Bennett BD, Collier HA, Cross JR, Fantin VR, Hedvat CV, Perl AE, Rabinowitz JD, Carroll M, Su SM, Sharp KA, Levine RL, Thompson CB (2010) The common feature of leukemia-associated IDH1 and IDH2 mutations is a neomorphic enzyme activity converting alpha-ketoglutarate to 2-hydroxyglutarate. *Cancer Cell* 17: 225–234
- Weis SM, Cheresch DA (2011) Tumor angiogenesis: molecular pathways and therapeutic targets. *Nat Med* 17: 1359–1370
- Wise DR, Ward PS, Shay JE, Cross JR, Gruber JJ, Sachdeva UM, Platt JM, DeMatteo RG, Simon MC, Thompson CB (2011) Hypoxia promotes isocitrate dehydrogenase-dependent carboxylation of alpha-ketoglutarate to citrate to support cell growth and viability. *Proc Natl Acad Sci USA* 108: 19611–19616
- Xu YF, Lu W, Rabinowitz JD (2015) Avoiding misannotation of in-source fragmentation products as cellular metabolites in liquid chromatography-mass spectrometry-based metabolomics. *Anal Chem* 87: 2273–2281